Atmospheric Research 161–162 (2015) 82–92

Contents lists available at ScienceDirect

Atmospheric Research

journal homepage: www.elsevier.com/locate/atmos

Subway construction activity influence on polycyclic aromatic hydrocarbons in fine particles: Comparison with a background mountainous site

Shaofei Kong [a,b,*], Xuxu Li [b], Qi Li [b], Yan Yin [a,b,*], Li Li [b], Kui Chen [b], Dantong Liu [c], Liang Yuan [b], Xiaobing Pang [a,b]

[a] Collaborative Innovation Center on Forecast and Evaluation of Meteorological Disasters, Key Laboratory for Aerosol-Cloud-Precipitation of China Meteorological Administration, Nanjing University of Information Science and Technology, Nanjing 210044, China
[b] Colloge of Atmospheric Physics, Nanjing University of Information Science & Technology, Nanjing 210044, China
[c] School of Earth, Atmospheric and Environmental Science, University of Manchester, Manchester, UK

ARTICLE INFO

Article history:
Received 30 November 2014
Received in revised form 30 March 2015
Accepted 7 April 2015
Available online 17 April 2015

Keywords:
$PM_{2.5}$
Polycyclic aromatic hydrocarbons
Subway construction activities
Background mountainous site
Source identification
Health risk

ABSTRACT

Intensive construction activities worsened the surrounding atmospheric environment in China. Eighteen polycyclic aromatic hydrocarbons (PAHs) in fine particles ($PM_{2.5}$) were collected at a subway construction site (SC) of Nanjing and compared with a regional background mountainous site (BM) to examine the influence of anthropogenic activities on concentrations, sources and health risks of PAHs. Average PAH concentrations at SC were higher than BM at a factor of about 5.9. All PAH species at SC were higher than BM, with the SC/BM ratios ranging from 1.3 (NaP) to 10.3 (BaP). PAH profiles differed for the two sites. The SC site had higher mass fractions of PAHs from coal combustion and vehicle emission, while the BM site held higher mass percentages of PAHs from long-range transported wood combustion and industrial activities. Lower temperature at BM may lead to the higher mass percentages of low ring PAHs. Coal combustion, traffic emissions and biomass burning were the common sources for PAHs at both SC and BM. Construction workers were exposed to higher BaPeq concentrations, nearly ten times of the background site and their lifetime cancer risk reached to 0.6 per 1,000,000 exposed worker, owing to the influence of coal combustion, vehicle emission and industrial activities at the surroundings of SC.

1. Introduction

Polycyclic aromatic hydrocarbons (PAHs), formed due to incomplete combustion or pyrolysis of organic material, are a type of organic compounds with high carcinogenicity and mutagenicity. For PAHs in fine particles ($PM_{2.5}$), various source apportionment studies indicated that the major sources are coal combustion, vehicle emission and petroleum in China (Gu et al., 2010; Tan et al., 2011; Li et al., 2014b; Wu et al., 2014a). Meanwhile, PAHs in road dust have also been widely recognized (Yang et al., 1999; Murakami et al., 2005; Han et al., 2009; Zhao et al., 2009). Construction activities including laying foundations, paving road, decorating, and transporting construction materials and wastes emit not only dust, but also particulate and gaseous air pollutants from highly concentrated non-road engines and on-road vehicles. Subramanyam et al. (1994) observed that the presence of construction activities near the sampling site can affect the concentration levels of PAHs. It indicated that the surrounding environment of the construction site is a type of hot-spot sites for PAHs in fine particles and should be paid attention from the view of protecting the health of construction workers or human living near these sites.

Due to the urbanization, construction of urban rail transit system including subway and main roads is now springing out in many megacities of China. According to the National Economic and Social Development of the Twelfth Five Year Plan Outline, the urban rail transit system is in vast development plan (http://www.gov.cn/2011lh/content_1825838_2.htm). Till September 2013, 37 cities have been authorized to construct subways, including most of the megacities, such as Beijing, Tianjin, Shanghai, Guangzhou, Nanjing and Shenzhen (http://finance.chinanews.com/cj/2013/11-25/5542506.shtml). These cities mainly locate at regions with serious haze and $PM_{2.5}$ pollution frequently occurred, such as Beijing–Tianjin–Hebei (Zhao et al., 2013), Yangtze River Delta (YRD) (Ding et al., 2013), Pearl River Delta (Tan et al., 2009, 2011), Sichuan Basin (Tao et al., 2014), Shandong peninsula (Wang et al., 2014), city clusters of central China (Geng et al., 2013), Guanzhong Plain (Wang et al., 2015a), northeast China (Liu et al., 2015) and west-Taiwan Strait (Deng et al., 2014). In addition, the subway construction sites are in close proximity to urban main roads with intense traffic flows. The subway construction sites are surrounded by major sources of PAHs in $PM_{2.5}$, including road dust (Yang et al., 1997, 1999; Zhao et al., 2009) and vehicles of both diesel (Liang et al.,

* Corresponding authors at: Nanjing University of Information Science and Technology, Ningliu Road 219, Nanjing, China. Tel./fax: +86 25 58731207.
E-mail addresses: kongshaofei@126.com (S. Kong), yinyan@nuist.edu.cn (Y. Yin).

http://dx.doi.org/10.1016/j.atmosres.2015.04.004
0169-8095/

2006; Wu et al., 2014b) and gasoline (Elghawi et al., 2010; Wu et al., 2014b). Yang et al. (1997) found that the highest PAH content in road dust from the urban area is located at the aerodynamic particle diameter of 1.8 μm. And dust deposited on the roads can be easily resuspended into the air by traffic turbulence. Contributions of 42% and 36% from diesel and gasoline vehicles were obtained for PAHs in $PM_{2.5}$ at a roadside environment in Beijing (Wu et al., 2014b). Wu et al. (2014b) indicated that the control of construction activities in Beijing is one of the effective measures to improve air quality and also reduced PAH concentrations in $PM_{2.5}$ at a roadside environment were observed during the 2008 Olympic Games period. Therefore, the subway construction activities may deteriorate the surrounding air and raise health risks to workers or people living near the construction sites.

In the past decade, the gas/particle distribution (Ma et al., 2011; Wang et al., 2011; Xia et al., 2013; Zhang et al., 2013b), size distribution (Bi et al., 2005; Duan et al., 2005, 2007; Zhou et al., 2005; Wang et al., 2008), seasonal variation (Zhou et al., 2005; Huang et al., 2006; Tan et al., 2006; Hong et al., 2007; Wang et al., 2011, 2015b; Li et al., 2013a; Zhang et al., 2013a; He et al., 2014; Wu et al., 2014b), spatial variation in city scale (Wu et al., 2005, 2014a; Wang et al., 2006, 2008; Gao et al., 2012; Hu et al., 2012; Xia et al., 2013; He et al., 2014) or regional scale (Wang et al., 2011; Zhang et al., 2013b), vertical distribution (Li et al., 2005; Tao et al., 2007) and health risk of PAHs (Xia et al., 2013; Leung et al., 2014) in the atmosphere have been widely investigated in China. These investigations are conducted in both the northern cities—Harbin (Ma et al., 2010), E'erduosi (Wu et al., 2014a), Beijing (Okuda et al., 2002, 2006, 2011; Zhou et al., 2005; Huang et al., 2006; Wang et al., 2008; Ma et al., 2011; Li et al., 2013a; Leung et al., 2014; Wu et al., 2014b), Tianjin (Wu et al., 2005; Shi et al., 2014), Xi'an (Leung et al., 2014), Taiyuan (Xia et al., 2013; Li et al., 2014a) and Zhengzhou (Wang et al., 2015b) and the southern cities—Shanghai (Wang et al., 2014), Nanjing (Wang et al., 2006; He et al., 2014), Hangzhou (Okuda et al., 2002), Fuzhou (Zhang et al., 2013a), Xiamen (Hong et al., 2007; Leung et al., 2014), Chongqing (Okuda et al., 2002), Guiyang (Hu et al., 2012), Guangzhou (Bi et al., 2002, 2005; Duan et al., 2005, 2007; Li et al., 2005; Tan et al., 2006, 2011; Gao et al., 2011, 2012; Leung et al., 2014), Shenzhen (Sun et al., 2015) and Hong Kong (Lee et al., 2001; Leung et al., 2014). To sum up, PAHs in particulate matter exhibited highest concentrations in winter and lowest concentrations in summer (Zhou et al., 2005; Huang et al., 2006; Tan et al., 2006; Wang et al., 2011; Li et al., 2013a; Xia et al., 2013; Zhang et al., 2013a; He et al., 2014; Wu et al., 2014b). For spatial variation, they hold higher concentrations at the roadside environment (Wang et al., 2006; Wu et al., 2014b) or industrial sites (Wu et al., 2014a) or rural sites (Wang et al., 2008, 2011) where obvious sources of them are highly concentrated, such as automobile exhausts, industrial plants and domestic heating/cooking stoves, respectively. For size distribution, most PAHs are mainly associated with fine particles (Bi et al., 2005; Duan et al., 2005; Zhou et al., 2005; Wang et al., 2008; Sun et al., 2015). Recently, Leung et al. (2014) found that the human bronchial epithelial cells exposed to the extracts of PAHs in $PM_{2.5}$ collected in five Chinese megacities demonstrated significant migratory activities, indicating an increase of tumorigenicity. Therefore, the investigation of PAHs in fine particles at sites with obvious emission sources is of great importance, from the view of protecting human health. However, few studies have addressed the concentrations of PAHs in $PM_{2.5}$ at hotspot sites such as the surroundings of subway construction activities till now.

Nanjing, as one of the three central cities of YRD, is the host city for the 2014 Youth Olympic Games. Six subway lines were constructed at the same time to meet the transport needs from the year of 2012. It is an ideal site to study the influence of subway construction activities on the chemical compositions of $PM_{2.5}$. Detailed investigations of atmospheric $PM_{2.5}$ are conducted at a subway construction site (SC) during its foundation dredging period. At this period, more vehicles are used for excavation and transportation of construction materials and wastes. For clearly identifying the pollution levels, sources and health risks of PAHs at the subway construction site, a comparative sampling campaign was immediately organized at a remote mountainous (BM) site of YRD—Mt. Huang (1864 m). It is 220 km away from the southeast of Nanjing and is the background reference site of YRD with negligible local anthropogenic sources (Chen et al., 2014).

The main objectives of this study are to: (1) obtain the levels of PAHs in $PM_{2.5}$ at the subway construction site and compare them with the background mountainous site; (2) analyze the influence of sources and meteorological parameters on PAHs in the two sites; and (3) calculate the lifetime health risks by exposure to PAHs in $PM_{2.5}$ for construction workers.

2. Methodology

2.1. $PM_{2.5}$ collection

Daily 24 h $PM_{2.5}$ samples were collected with a sampler (TH-150C, Wuhan Tianhong Ltd., China) at a flow rate of 100 L/min on the rooftop (6 m high) of a guard room of Nanjing University of Information Science & Technology (NUIST). The sampling time lasted from June 14 to July 9, 2013, covering the whole foundation dredging period. The starting time is from about 08:00 am each day. NUIST locates at the suburban of Nanjing, with a steel factory 2 km to the east of the campus and a chemical industry park about 10 km to the northeast. The sampling site faces one road (about 10 m in the east direction) with heavy traffic and the subway is constructed on this road as Fig. 1 shows. Daily 24 h $PM_{2.5}$ samples were collected at Mt. Huang during Oct. 16-Nov. 02, using the same equipment. Mt. Huang is situated in Anhui Province, southeastern China, with an area of 40×30 km^2. The sampling site is set at the summit with an altitude of 1840 m (Fig. 1). The annual average rainfall at the summit is 2369 mm and the average frequency of rainfall is 181 days. With limitation on equipment, the sampling between the two sites was not simultaneous. It should be noted that $PM_{2.5}$ at summer and autumn periods is low in China with less heating activities compared to winter (Li et al., 2014b). And He et al. (2014) found that the PAHs in $PM_{2.1}$ at suburban and urban sites of Nanjing both decreased in winter > spring > autumn > summer. Therefore, the sampling design for the two sites in this study can be accepted. At rainy days, $PM_{2.5}$ was not collected. 17 and 16 samples were obtained for the construction site and Mt. Huang, respectively. Quartz fiber filters (Whatman Company, UK, Ø 90 mm, baked at 800 °C for 2 h) were adopted. After sampling, the filters were sealed in aluminum foil envelopes until weighing. The filters were weighed before and after sampling under a constant temperature (22 °C) and relative humidity (35%) controlled environment by a microbalance (Ohaus Discovery DV214CD) with sensitivity of ±0.010 mg. Then they were stored at −20 °C until chemical analysis.

2.2. PAH analysis and suitability analysis of the data set

For PAH analysis, filters are extracted ultrasonically with dichloromethane, then concentrated using a rotary evaporator, purified with a silica gel and re-concentrated by rotary evaporation. Finally they were condensed to exactly 1 mL under a gentle nitrogen stream in 60 °C water bath. The extracts were transferred into two ampoule bottles and stored in a refrigerator until analysis. Gas chromatography coupled to mass spectrometry (GC–MS) was used according to the EPA Method TO-13A. For each sample, the procedures of sampling, pretreatment and analysis were completed within one month. PAHs in the final extracts were analyzed with a trace 2000 GC–MS (Thermo Finnigan, USA) apparatus with selected ion monitoring (SIM). Detailed analysis of GC–MS could be found in our former works (Kong et al., 2012; Wu et al., 2014a).

Quantification of PAHs is standardized by the retention times and peak areas of the calibration standards. Internal standard method is adopted. 1000 mg/L reserve liquid including Perylene-d12,

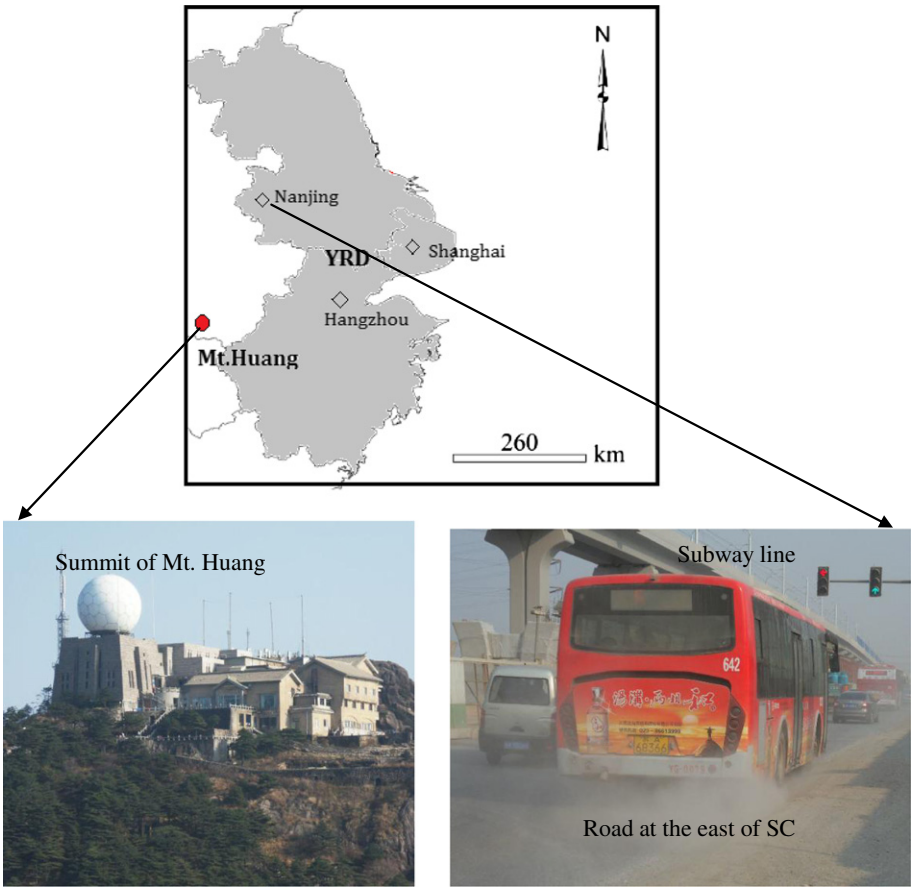

Fig. 1. Locations of Nanjing and the background mountainous site of Mt. Huang (BM). YRD indicates Yangtze River Delta region and is shown in gray. Location of the subway construction site (SC) is on the rooftop of a guard room, 6 m high and about 10 m from the subway construction line. At the summit of Mt. Huang (altitude as 1840 m), there is a meteorological observatory base. Sampling is conducted on the rooftop of a building, about 10 m high.

Chrysene-d12, Acenaphthene-d12, Naphthalene-d8 and Phenanthrene-d10 is diluted by n-hexane to 20 mg/L and stored below 4 °C. It is used as the internal standard solution. 18 kinds of PAHs are analyzed including naphthalene (NaP), acenaphthylene (Acy), acenaphthene (Ace), fluorene (Fl), phenanthrene (Phe), anthracene (Ant), fluoranthene (Flu), pyrene (Pyr), benzo[a]anthracene (BaA), chrysene (Chr), benzo[b] fluoranthene (BbF), benzo[k]fluoranthene (BkF), benzo[a]pyrene (BaP), Benzo(e)pyrene (BeP), dibenz[a,h]anthracene (DBA), indeno [1,2,3-cd]pyrene (InP), benzo[ghi]perylene (BghiP) and coronene (Cor). The recovery test is performed by spiking known amounts of a mixture of PAHs and then the spiked filter is treated the same way as mentioned above. The recoveries for each PAH fell between 86% and 95%, and the relative standard deviation is less than 10%. The detection limits for the 18 kinds of PAHs are in the range of 3.0–10.0 ng. PAHs can be classified by their numbers of aromatic ring as follows: 2-ring including Nap; 3-ring including Acy, Ace, Fl, Phe and Ant; 4-ring including Flu, Pyr, BaA and Chr; 5-ring including BbF, BkF, BaP and BeP; 6-ring including InP, DBA and BghiP; and 7-ring including Cor. They can also be further classified into lower molecular weight (LMW) containing 2 and 3-ring PAHs, middle molecular weight (MMW) containing 4-ring PAHs and higher molecular weight PAHs (HMW) containing 5-, 6- and 7-ring PAHs.

Sampling artifacts may exist for lower ring PAHs. Hart and Pankow (1990) indicated that volatilization losses from particle laden filters, adsorption from the gas phase to the filters themselves, and chemical reactions on the particle laden filter are three most important mechanisms of sampling artifacts for PAH studies. Filippo et al. (2010) indicated that volatilization of PAHs is not a serious artifact for compounds with vapor pressures less than that of fluoranthene. Kavouras et al. (1999) found that adsorption of gas-phase organic compounds onto glass and quartz filters can result in an overestimation of the particulate phase concentrations and these positive artifacts can be 10–35% for ambient atmospheres. Tsapakis and Stephanou (2003) pointed out that the chemical reactions of PAHs with oxidants during high-volume sampling were suspected as a potential source of artifacts. The sampling artifact issue is mainly concerned for gas/particle distribution studies of PAHs (Mandalakis et al., 2002; Tsapakis and Stephanou, 2003; Vardar et al., 2004; Wang et al., 2011; Ma et al., 2011; Mu et al., 2014) by high-volume filter/sorbent sampling which is thought to suffer from artifacts caused by the rapid exchange of PAH mass between particle-loaded filters and the incoming gas phase (Galarneau, 2008). Therefore, the present data set here is suitable for detailed discussion of PAH concentrations in fine particles, with a medium sampling flow rate (100 L/min) and quartz filter used.

2.3. Meteorological data

Meteorological parameters including temperature, relative humidity (RH), wind speed, wind direction and visibility (Vs) are recorded by the meteorological observatory base in the campus of NUIST (http://qxt.nuist.edu.cn/) which is about 1.5 km from the sampling site. At Mt. Huang, the meteorological data are monitored by a local meteorological station at the summit of it. As listed in Table 1, the average temperature at SC is 28.7 °C, about three times of that at Mt. Huang. The averaged RH is similar for the two sites.

Table 1
Statistic of meteorological parameters for the subway construction site (SC) and Mt. Huang.

Sites	Elevation (m)	T[a] (°C)	RH[b] (%)	Wind speed (m s^{-1})	Wind direction (°)	Visibility (km)
Mt. Huang	1840	9.6 ± 3.7	65 ± 33	5.4 ± 2.3	229 ± 74	19.3 ± 11.3
SC	461	28.7 ± 2.6	64 ± 9	2.7 ± 0.7	165 ± 58	9.9 ± 4.9

[a] Temperature.
[b] Relative humidity.

2.4. Data processing

2.4.1. Coefficient of divergence

In order to identify the differences of PAH composition profiles in $PM_{2.5}$ at the two sites, coefficient of divergence is used to measure the spread of the data points for two data sets. It is determined as follows:

$$CD_{jk} = \sqrt{\frac{1}{p}\sum_{i=1}^{p}\left(\frac{x_{ij}-x_{ik}}{x_{ij}+x_{ik}}\right)^2}$$

where j and k stand for the two profiles of the sampling sites, p is the number of investigated PAHs, 18 in this study, and x_{ij} and x_{ik} represent the average mass concentrations of PAH species i for j and k. If CD_{jk} approaches zero, PAH composition profiles are similar, and if it approaches one, they are significantly different (Wu et al., 2014a). For calculating the CD_{jk} values, normalized PAH mass fractions to total PAHs were used.

2.4.2. Principal component analysis

Source apportionment for PAHs in $PM_{2.5}$ at SC and Mt. Huang is done by principal component analysis (PCA). PCA is executed by the varimax rotated factor matrix method, based on the orthogonal rotation criterion which maximizes the variance of the squared elements in the column of a factor matrix, using statistical software (SPSS 13.0). Factor loadings indicate the correlation of each pollutant species with each component and are related to the source emission composition.

2.4.3. Health risk assessment of PAHs

Health risk estimation can be calculated using PAH exposure through inhalation of air particles (Li et al., 2013b; Wiriya et al., 2013; Jamhari et al., 2014). The incremental lifetime cancer risk (ILCR) for humans can be determined by calculating the lifetime average daily dose (LADD) of PAHs. The equations used for estimating LADD and ILCR are widely used in the former studies (Li et al., 2013b; Wiriya et al., 2013; Jamhari et al., 2014) as:

$$LADD = C \times IR \times ED \times EF/(BW \times ALT) \quad (1)$$

$$ILCR = LADD \times CSF \quad (2)$$

where C is the mass concentration of PAHs in $PM_{2.5}$ (mg m^{-3}); IR is the inhalation rate (m^3 day^{-1}, 20 for adult); ED is the lifetime exposure duration (52 years for adult); EF is the exposure frequency (250 days $year^{-1}$, except for holidays and weekends); BW is the body weight (70 kg for adult); ALT is the averaging lifetime for carcinogens (70 years × 365 days $year^{-1}$ = 25,550 days); and CSF is the cancer slope factor (per mg kg^{-1} day). In this study, CSF value for BaP from inhalation is selected as 3.14 (mg kg^{-1} $day^{-1})^{-1}$ and the total BaP equivalent (BaPeq) concentration is used to calculate LADD instead of PAH mass concentrations (Jamhari et al., 2014). BaPeq is calculated by multiplying the mass concentrations of each PAH species of their corresponding toxic equivalency factors (TEFs) as Eq. (3) (Wiriya et al., 2013):

$$\begin{aligned}BaPeq = {} & 0.001(NaP + Ace + Flu + Phe + Fl + Pyr) \\ & + 0.01(Ant + Chr + BghiP) + 0.1(BaA + BbF + BkF + InP) \\ & + BaP + DBA. \end{aligned} \quad (3)$$

3. Results and discussion

3.1. Differences of PAH concentrations between the subway construction and background mountainous sites

Statistics of PAHs at the subway construction site and Mt. Huang are listed in Table 2. The average PAH in $PM_{2.5}$ at SC was 9.02 ng m^{-3}, 5.9 times of that for PAHs in $PM_{2.5}$ at Mt. Huang (averaged as 1.53 ng m^{-3}). All PAH species were higher than those at Mt. Huang, with the SC/BM ratios varying in 1.3 (NaP)–10.3 (BaP). LMW-PAHs, MMW-PAHs and HMW-PAHs elevated by 2.8, 3.2 and 7.5 times, respectively (Fig. 2). At BM, the L-PAH/H-PAH ratio was 0.43, two times of that for SC. The main reason may be that the lower temperature at BM (averaged as 9.6 °C) can promote more L-PAHs adsorbing on particle phase than those for MMW-PAHs and HMW-PAHs (Esen et al., 2008;

Table 2
Statistics of PAHs in $PM_{2.5}$ at Mt. Huang and the subway construction site of Nanjing (ng m^{-3}).

	Mt. Huang (BM, n = 16)				Subway construction site (SC, n = 17)			
	Mean	SD	Min	Max	Mean	SD	Min	Max
NaP	0.09	0.02	0.03	0.12	0.12	0.04	0.05	0.19
Ace	0.02	0.00	0.02	0.03	0.04	0.02	0.02	0.07
Acy	0.02	0.00	0.01	0.02	0.05	0.02	0.02	0.09
Fl	0.03	0.01	0.01	0.05	0.23	0.07	0.11	0.45
Phe	0.10	0.07	0.02	0.32	0.55	0.33	0.21	1.75
Ant	0.02	0.00	0.02	0.03	0.11	0.13	0.02	0.60
Flu	0.14	0.12	0.02	0.53	0.45	0.26	0.11	1.03
Pyr	0.12	0.10	0.02	0.41	0.47	0.38	0.11	1.65
BaA	0.04	0.03	0.02	0.13	0.36	0.27	0.08	1.24
Chr	0.14	0.10	0.03	0.40	0.54	0.33	0.09	1.20
BbF	0.18	0.14	0.03	0.58	1.39	0.96	0.32	4.39
BkF	0.06	0.04	0.03	0.15	0.46	0.40	0.09	1.63
BaP	0.07	0.05	0.03	0.18	0.70	0.44	0.20	2.02
BeP	0.13	0.09	0.03	0.34	0.86	0.63	0.22	2.79
DBA	0.03	0.01	0.02	0.08	0.28	0.22	0.03	0.98
InP	0.12	0.10	0.02	0.45	0.90	0.62	0.26	2.74
BghiP	0.14	0.12	0.02	0.54	0.99	0.70	0.28	3.11
Cor	0.08	0.07	0.05	0.31	0.55	0.34	0.19	1.39
LMW-PAHs	0.28	0.09	0.14	0.54	1.09	0.50	0.43	2.75
MMW-PAH	0.44	0.34	0.11	1.43	1.82	1.15	0.41	4.38
HMW-PAHs	0.81	0.58	0.25	2.63	6.12	4.08	1.61	18.62
COMPAHs	0.89	0.63	0.25	2.31	5.34	3.36	1.37	15.10
C-PAHs	0.64	0.43	0.22	1.86	4.63	2.98	1.13	13.76
PAHs	1.53	0.92	0.55	3.70	9.02	5.27	2.63	24.10

Lower molecular weight (LMW) contains 2 and 3-ring PAHs, middle molecular weight (MMW) contains 4-ring PAHs and higher molecular weight PAHs (HMW) contains 5-, 6- and 7-ring PAHs. COMPAHs: combustion derived PAHs including Flu, Pyr, Chr, BbF, BkF, BaA, BeP, BaP, InP and BghiP. C-PAHs: carcinogenic PAHs including BaA, BbF, BkF, BaP, InP and DBA.

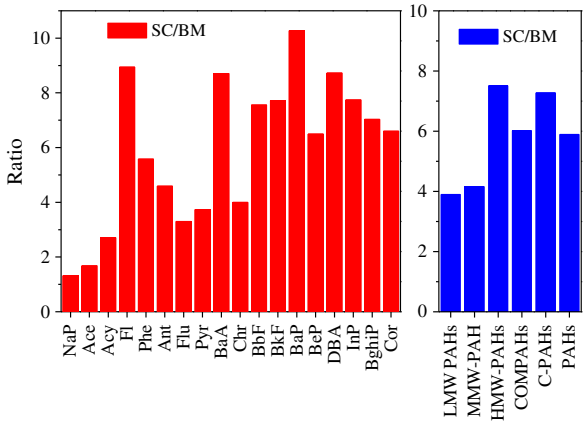

Fig. 2. Comparison of PAH species between the subway construction site (SC) and the regional background mountainous site—Mt. Huang (BM).

Filippo et al., 2010; Ma et al., 2011). It was verified by the weak negative correlations between LMW-PAHs and temperatures for the two sites (Table 3). With limited sampling periods, no significant correlations for wind speed and RH with PAH concentrations are found in this study. It should be noted that RH can influence the gas/particle distribution of PAHs (Mader and Pankow, 2001) and negative correlations were found between individual PAHs with wind speed, indicating the dilution effect of atmospheric turbulence on pollutant concentrations (Tan et al., 2006). Li et al. (2012) also found abundant LMW-PAHs in Mt. Hua (2060 m) air and attributed it to the increased transformation of gaseous species to the solid phase due to lower temperature of the mountaintop atmosphere. Meanwhile, more pyrogenic PAHs from fossil fuel combustion can also lead to the lower L-PAH/H-PAH ratio at SC (Hassanien and Latif, 2008).

The COMPAHs (combustion-derived PAHs including Flu, Pyr, Chr, BbF, BkF, BaA, BeP, BaP, InP and BghiP) (Bourotte et al., 2005; Kong et al., 2011) and C-PAHs (carcinogenic PAHs including BaA, BbF, BkF, BaP, DbA and InP) increased by 5.1 and 6.3 times. It suggests that the surrounding environment of the subway construction site is influenced more significantly by combustion sources and is more harmful to human health. BaP, BaA, Fl, DBA, InP, BghiP, BbF and BkF exhibited higher SC/BM ratios, indicating the enhanced emissions from vehicles, coal combustion and industrial activities. As InP and BghiP are always considered as tracers of gasoline vehicles (Wu et al., 2014a, 2014b) and highly correlated in this study ($R^2 = 0.97$ and 0.99 for BM and SC, respectively); BaP and InP are markers for sinter and industrial boilers, and DBA can be a signature for power plants with coal as fuel (Kong et al., 2013); BkF is one of the markers for iron smelt (Yang et al., 2002). Chen et al. (2013) observed that BghiP, InP, BkF, BaA and Chr hold higher emission factors for both gasoline and diesel vehicles at an urban tunnel in Nanjing. The results are in accordance with the surrounding environment of SC as discussed in Section 2.1.

From literatures, studies related with PAHs at construction sites are limited and comparison could not be done. The PAH concentrations at Mt. Huang are lower than those at Mt. Hua (averaged as 7.9 ng m^{-3} for particles with diameter less than 2.1 μm) (Li et al., 2012) and Mt. Tai (averaged as 58 ng m^{-3} for particles with diameter less than 9.0 μm) (Wang et al., 2009) (Table 4). It should be indicated that the study at Mt. Hua is in winter when biofuel combustion plus plant emission and fossil fuel combustion are more abundant in northern China. They are the main influence sources for PAHs at Mt. Hua. For Mt. Tai, it is located at the center of Shandong peninsula and surrounded by intensive industrial and power plants which can explain the highest PAH concentrations at the summit of it, in the view of regional transport of air pollutants. From Table 2, it can also find that PAH concentrations at the elevated sites of China are much higher than those in Europe (Lammel et al., 2009; Masiol et al., 2013), Canada (Choi et al., 2009), Northern Algeria (Ladji et al., 2009) and Korea (Lee et al., 2008). It implied that even at the mountainous background site of China, PAHs exhibited higher concentrations and the control of PAH pollution in China is urgent.

Fig. 3 shows that the CD value between SC and BM was 0.27, indicating a difference in PAH composition. The difference was mainly driven by Chr, Flu, Pyr, NaP, Ace, Acy and Ant at BM, with higher mass percentages, consistent with the long-range transport wood combustion markers such as Ant, Phe, Flu and Pyr or NaP and Ant (Khalili et al., 1995). The higher mass percentages of Ace, Acy and Ant at BM also suggested the influence of long-range transport industrial processes which are signatures for cement plant (Yang et al., 1998). For SC, the higher mass percentages of other PAHs reflected the influence of coal combustion, vehicle emission and industrial activities. Li et al. (2012) concluded that biofuel combustion was most important for PAHs in

Table 3
Correlations between meteorological parameters and different rings of PAHs at Mt. Huang and SC.

	R2	R3	R4	R5	R6	R7	WS	T	RH
R2	1	0.722(**)	0.426	0.321	0.263	0.331	−0.029	−0.434	0.236
R3	0.586(*)	1	0.263	0.182	0.137	0.192	−0.087	−0.324	0.193
R4	0.36	0.847(**)	1	0.898(**)	0.875(**)	0.856(**)	−0.301	−0.658(**)	0.4
R5	0.225	0.485	0.829(**)	1	0.978(**)	0.928(**)	−0.314	–	0.4
R6	0.124	0.174	0.588(*)	0.935(**)	1	0.963(**)	−0.299	−0.44	0.39
R7	−0.008	0.2	0.607(*)	0.911(**)	0.938(**)	1	−0.355	−0.458	0.338
WS	0.208	0.04	0.022	−0.119	−0.183	−0.228	1	0.161	−0.551(*)
T	−0.21	−0.441	−0.418	−0.02	0.234	0.163	−0.583(*)	1	−0.453
RH	0.008	0.186	0.045	−0.045	−0.103	−0.057	0.244	−0.137	1

The upper trigonal matrix is for SC (with light gray shading) and the down trigonal matrix is for Mt. Huang.
**Correlation is significant at the 0.01 level (2-tailed).
*Correlation is significant at the 0.05 level (2-tailed).
WS—wind speed, m s^{-1}.
T—temperature, °C.
RH—relative humidity, %.
R2–R7 indicate 2-ring, 3-ring, 4-ring, 5-ring, 6-ring and 7-ring PAHs, respectively.

Table 4
Comparison of PAH concentrations (ng m^{-3}) at elevated sites around the world.

Sites (altitude, m)	Sampling periods	Particle size	Types of PAHs detected	Concentrations	References
Mt. Huang (1840)	Autumn	$PM_{2.5}$	18	0.55–3.7	This study
Mt. Halla (1100)	March 1999 to March 2002	$PM_{2.5}$	23	0.045–2.93	Lee et al. (2008)
Mountains of Western Canada (570–2902)	2003–2004	Collected by XAD-resin based PAS	4	0.016–1.03	Choi et al. (2009)
Chréa mountain (1500)	Oct. 2006	$PM_{0.95-10}$	20	0.142	Ladji et al. (2009)
Zugspitze, Alps (2670)	Summer 2007 and winter 2008	Gas and particle	24	0.079–1.30	Lammel et al. (2009)
Mt. Tai (1534)	June 2006	$PM_{9.0}$	17	58	Wang et al. (2009)
Mt. Hua (2060)	Winter, 2009	PM_{10}	15	7.3 ± 3.4	Li et al. (2012)
		$PM_{2.1}$		7.9 ± 2.1	
		$PM_{2.1-9.0}$		0.8 ± 0.4	
		$PM_{0.95}$		0.37	
Alpine pass (2020)	Jan.–Dec., 2011	PM_{10}	8	0.1–3.9	Masiol et al. (2013)

aerosols at Mt. Hua (2060 m) which was different from Chinese urban area. Meanwhile, the much lower temperature at BM can lead to higher adsorption of these lower ring PAH species on particles by quartz filter sampling which may also explain the higher mass percentages of them at BM.

3.2. Ring distribution

Fig. 4 shows the ring distribution of PAHs at BM and SC, both dominated by 4-ring and 5-ring PAHs, followed by 6-ring and 3-ring in a second order. For mass percentage comparison, 5-ring and 6-ring PAHs at SC were higher than those at BM. While for 4, 3 and 2-ring PAHs, they were lower at SC. PAHs with 3 or 4 rings are semi-volatile and partition significantly in both gas and particle phase, and high ring PAHs mostly reside in particle phase (Huang et al., 2006). Possanzini et al. (2004) indicated that more than 90% of 2- and 3-ring PAHs are found in the gas phase, while congeners with more than 4 rings are present almost entirely in the particle phase. As discussed before, the lower temperature at BM favored the transformation of gaseous PAHs with low rings to particle phase (Li et al., 2012), and this can explain the higher mass percentages of the low-ring PAHs. However, the mass concentrations of 2-ring and 3-ring PAHs are higher at the urban site—SC than the background site—Mt. Huang, it indicated that there are more sources for them at SC, such as the petroleum evaporation.

PAHs (3 + 4) and PAHs (5 + 6) behave quite differently due to their chemical characteristics and nonvolatile PAHs are more efficiently removed from the atmosphere than semi-volatile PAHs by the photochemical degradation (Tan et al., 2011). The ratio at SC was 0.55 ± 0.15, much lower than that for BM of 0.92 ± 0.27 (independent t-test, $P < 0.001$) (Fig. 5a), indicating that PAHs at BM may suffer from more enhanced photochemical degradation processes. Meanwhile the emission sources can also influence the PAH (3 + 4) and PAH (5 + 6) ratios. Former studies indicated that the ratio of PAHs (3 + 4)/PAHs (5 + 6) varied much for various sources, such as 0.53 for sinter (Kong et al., 2013), 0.59 for mixed vehicles (Chen et al., 2013), 0.81 for industrial boilers (Kong et al., 2013), 1.0 for coal-fired power plant (Kong et al., 2013) and 6.75 for biomass fuel combustion (Shen et al., 2013), respectively (Table 5). The SC site is located at the roadside and near a steel factory and industrial park which may lead to the lower ratio of PAHs (3 + 4)/PAHs (5 + 6) at this site. While for the remote site BM, local or long-range transported biomass burning may influence the aerosol more which can lead to the higher ratio of PAHs (3 + 4)/PAHs (5 + 6). Possanzini et al. (2004) indicated that for 4-ring PAHs (Flu, Pyr, BaA and Chr), their phase distributions are influenced obviously by temperature and in winter (temperature of 8 °C), their contents in gas phase decreased by 20%–50% when compared with those for autumn (temperature of 13 °C) and spring (temperature of 12 °C) periods. Therefore, the much lower temperature at BM (averaged as 9.6 °C) may increase the PAHs (3 + 4) on the particle phase, which can also explain the higher PAH (3 + 4)/PAH (5 + 6) values. From Table 5, it can be found that the PAH (3 + 4)/PAH (5 + 6) values for urban sites in megacities of China ranged from 0.25–1.96 and for background sites, they varied from 0.28–1.95. To conclude, the ratios can vary widely under the influence of emission sources and meteorological parameters. One interesting thing that should be noted is that when compared with the PAH (3 + 4)/PAH (5 + 6) ratios for southern Chinese cities like Guangzhou (Gao et al., 2012; Leung et al., 2014), Hong Kong (Leung et al., 2014), Shenzhen (Sun et al., 2015) and Xiamen

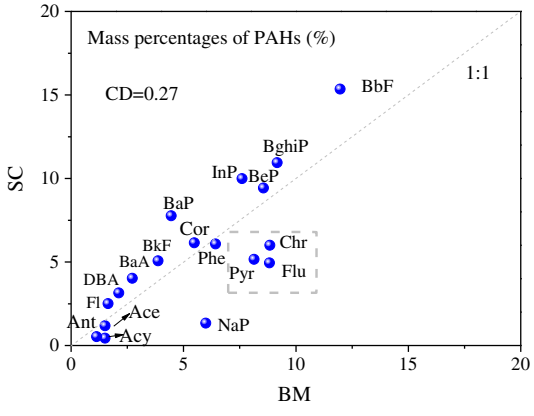

Fig. 3. Comparison of PAH mass percentages for the subway construction site (SC) and the regional background mountainous site—Mt. Huang (BM).

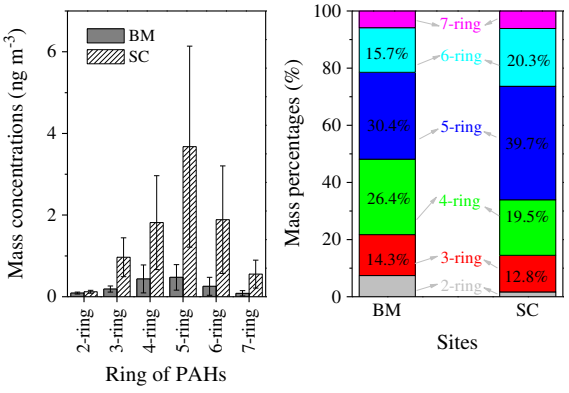

Fig. 4. Ring distribution of PAHs in $PM_{2.5}$ at the subway construction site (SC) and the regional background mountainous site—Mt. Huang (BM). The left is for mass concentrations (a) and the right is for mass percentages (b).

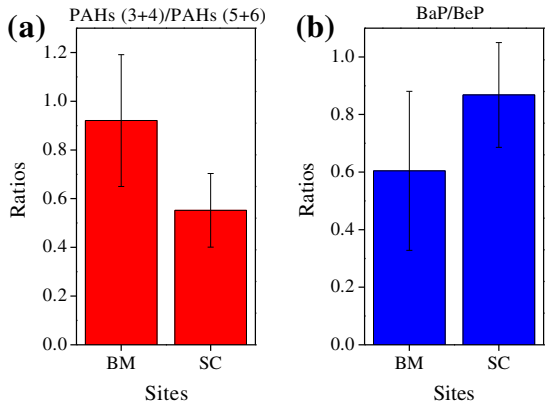

Fig. 5. Ratios of PAHs (3 + 4)/PAHs (5 + 6) (a) and BaP/BeP (b) for the subway construction site (SC) and the regional background mountainous site—Mt. Huang (BM).

(Leung et al., 2014), the values in Beijing (Wang et al., 2008; Leung et al., 2014) and Xi'an (Leung et al., 2014) are much higher. It indicated that coal and biomass burned for home heating during winter in northern China influenced PAHs obviously, according to the values for coal and biomass fuel combustion listed in Table 5.

Former studies indicated that BaP is labile to photochemical degradation while its isomer BeP is much stable, thus the ratio of BaP/BeP can be thought as an indicator of aerosol aging (Huang et al., 2006; Tan et al., 2009, 2011; Li et al., 2012). The BaP/BeP ratio at SC was 0.86 ± 0.18, higher (independent t-test, $P < 0.001$) than that for BM of 0.60 ± 0.28 (Fig. 5b), indicating an enhanced photochemical oxidation for PAHs at BM. Li et al. (2012) indicated that the ratio showed an

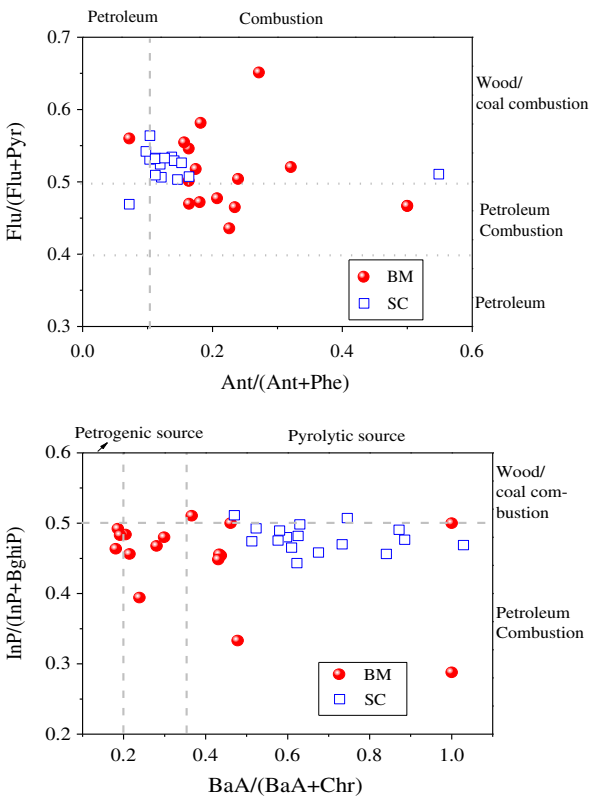

Fig. 6. Graphic illustration of the diagnostic ratios for the sources of PAHs.

Table 5
Ratios of PAHs (3 + 4)/PAHs (5 + 6) and BaP/BeP for various sources, urban sites and background sites.

Sources or sites	Particle size	PAHs (3 + 4)/PAHs (5 + 6)	BaP/BeP	References
Sources				
Joss paper burning	TSP	/	1.61	Rau et al. (2008)
Mixed vehicles	PM_{10}	0.59	–	Chen et al. (2013)
Coal-fired power plant	$PM_{2.5}$	1.0	0.50	Kong et al. (2013)
Sinter	$PM_{2.5}$	0.53	0.63	
Industrial boilers	$PM_{2.5}$	0.81	0.65	
Biomass fuel combustion	$PM_{1.1-2.1}$	6.75	1.31	Shen et al. (2013)
Urban sites				
Nanjing (SC)	$PM_{2.5}$	0.55	0.86	This study
Nanjing	$PM_{2.5}$	0.88	–	Wang et al. (2006)
Beijing	$PM_{2.5}$	1.45	–	Wang et al. (2008)
Guangzhou[a]	$PM_{2.5}$	0.25	0.64	Gao et al. (2012)
Beijing[b]	$PM_{2.5}$	/	0.83	Li et al. (2013a)
Nanjing	$PM_{2.1}$	0.86	0.78	He et al. (2014)
Beijing	$PM_{2.5}$	1.96	–	Leung et al. (2014)
Hong Kong	$PM_{2.5}$	0.51	–	
Guangzhou	$PM_{2.5}$	0.37	–	
Xiamen	$PM_{2.5}$	0.60	–	
Xi'an	$PM_{2.5}$	1.15	–	
E'erduosi[c]	$PM_{2.5}$	0.57	1.04	Wu et al. (2014a)
Shenzhen	$PM_{2.5}$	0.44	–	Sun et al. (2015)
Background sites				
Mt. Huang	$PM_{2.5}$	0.92	0.60	This study
Mt. Halla	TSP	/	0.34	Lee et al. (2008)
Guangzhou[d]	$PM_{2.5}$	0.28	0.75	Gao et al. (2012)
Mt. Hua	PM_{10}	/	0.5	Li et al. (2012)
E'erduosi[e]	$PM_{2.5}$	1.95	0.27	Wu et al. (2014a)

SC: the subway construction site in this study.
/: Values of PAHs are not listed or some 3-ring PAHs are not detected.
–: BeP is not detected.
[a] For a site in city center, with heavy traffic and busy commercial activities.
[b] For winter period, with large quantities of coal and biomass burned for home heating.
[c] For a central urban residential site.
[d] For a site 40 km northeast from urban center, located in a mountainous and hilly area with sparse population.
[e] For a background site, with 95% of the area covered by vegetation and no industrial sources.

Table 6
Factor loadings of PCA analysis for different rings of PAHs in $PM_{2.5}$ at Mt. Huang and a subway construction site (SC) of Nanjing.

	Mt. Huang			SC	
	Factor 1	Factor 2		Factor 1	Factor 2
R2	−0.061	**0.763**	R2	0.220	**0.902**
R3	0.205	**0.916**	R3	0.056	**0.932**
R4	0.643	0.687	R4	**0.908**	0.248
R5	**0.939**	0.324	R5	**0.975**	0.125
R6	**0.965**	0.042	R6	**0.987**	0.066
R7	**0.972**	−0.004	R7	**0.958**	0.137
% of variance	53.6	33.3	% of variance	61.9	29.7
Cumulative %	53.6	86.9	Cumulative %	61.9	91.7

Extraction method: principal component analysis.
Rotation method: Varimax with Kaiser Normalization.
Values higher than 0.7 are listed in bold.
R2–R7 indicate 2-ring, 3-ring, 4-ring, 5-ring, 6-ring and 7-ring PAHs, respectively.

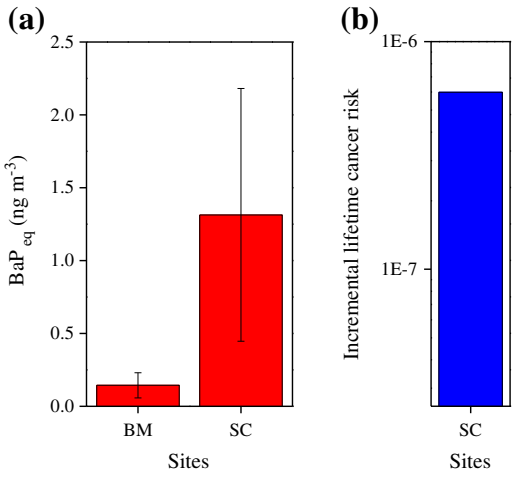

Fig. 7. Comparison of BaP equivalent (BaPeq) concentrations between the two sites (a) and incremental lifetime cancer risk (ILCR) for construction workers (b) exposed to PAHs in $PM_{2.5}$.

increasing trend with a decrease in altitude, which suggested an enhanced photochemical oxidation in the free troposphere. From Table 5, BaP/BeP ratios are lower for elevated mountainous sites (averaged as 0.48) than those for urban sites (averaged as 0.83). Meanwhile, the BaP/BeP ratios for particles directly emitted from a coal-fired power plant (Kong et al., 2013), sinter (Kong et al., 2013), industrial boilers (Kong et al., 2013), biomass fuel combustion (Shen et al., 2013) and joss paper burning (Rau et al., 2008) are 0.50, 0.63, 0.65, 1.31 and 1.61, respectively. It indicated that at BM, PAHs in particles suffered from obvious aging processes, especially for those emitted from biomass fuel combustion and joss paper burning.

3.3. Source identification

3.3.1. Diagnostic ratios

Fig. 6 illustrated widely used diagnostic ratios of Flu/(Flu + Pyr) vs. Ant/(Ant + Phe) and BaA/(BaA + Chr) vs. InP/(InP + BghiP) for identifying PAH sources. The ratio of Flu/(Flu + Pyr) appeared close to 0.40 for petroleum, between 0.40 and 0.50 for petroleum combustion, and higher than 0.5 for grass, wood or coal combustion (Gu et al., 2010; Tan et al., 2011). They were higher than 0.5 at SC, suggesting the dominance of wood/coal combustion. For the mountainous site BM, 38% of the samples held Flu/(Flu + Pyr) ratios of 0.4–0.5, indicating petroleum combustion. The ratio of Ant/(Ant + Phe) less than 0.1 is characteristic of petroleum, and the opposite is the combustion (Wang et al., 2008). In this study, only one sample at BM and SC exhibited values lower than 0.1, implying that combustion emission was the principal source for PAHs at the two sites. The InP/(InP + BghiP) ratios are reported to be 0.18, 0.37 and 0.56 for cars, diesel and coal, respectively (Tan et al., 2009). The ratios for SC and BM both concentrated in 0.4–0.5, implying that PAHs were dominated by both coal combustion and motor vehicles. There are some divergences for BM with InP/(InP + BghiP) values lower than 0.4, similar to the petroleum combustion derived from Flu/(Flu + Pyr) analysis. It was also validated by the BaA/(BaA + Chr) ratios, which were all higher than 0.37 at SC, suggesting pyrolytic source while for BM, some samples were from petrogenic source.

Table 7
Factor loadings of PCA analysis for PAHs in $PM_{2.5}$ at Mt. Huang and a subway construction site of Nanjing.

	Mt. Huang (BM)				Subway construction site (SC)		
	Factor 1	Factor 2	Factor 3		Factor 1	Factor 2	Factor 3
NaP	0.098	0.293	**0.643**	NaP	0.237	0.877	0.070
Ace	−0.098	−0.174	**0.814**	Ace	0.062	0.382	**0.783**
Acy	**0.968**	−0.099	0.207	Acy	0.126	**0.923**	0.024
Fl	**0.973**	−0.034	0.117	Fl	0.081	**0.956**	0.015
Phe	**0.968**	0.128	0.130	Phe	0.102	**0.904**	−0.085
Ant	**0.996**	−0.058	0.014	Ant	−0.030	0.306	**0.555**
Flu	0.318	**0.759**	**0.355**	Flu	**0.879**	0.322	0.018
Pyr	**0.966**	0.210	0.108	Pyr	**0.733**	0.319	−0.132
BaA	**0.987**	0.140	−0.032	BaA	**0.965**	0.042	0.145
Chr	0.706	**0.657**	0.144	Chr	**0.891**	0.200	0.022
BbF	−0.138	**0.959**	−0.122	BbF	**0.986**	0.107	0.091
BkF	**0.965**	0.230	−0.009	BkF	0.457	0.034	**0.462**
BaP	**0.910**	0.374	0.012	BaP	**0.966**	0.153	0.048
BeP	**0.860**	0.491	0.006	BeP	**0.984**	0.024	0.034
DBA	**0.996**	0.026	−0.051	DBA	**0.963**	0.115	0.063
InP	**0.904**	0.348	−0.146	InP	**0.990**	0.049	0.006
BghiP	**0.864**	0.434	−0.143	BghiP	**0.983**	0.017	0.028
Cor	**0.804**	0.490	−0.214	Cor	**0.950**	0.113	−0.096
% of Variance	67.0	17.3	7.8	% of Variance	55.4	21.6	6.7
Cumulative %	67.0	84.3	92.2	Cumulative %	55.4	77.1	83.9
Sources	Mixed coal combustion and vehicle emission	Biomass burning	Incense/joss paper burning	Sources	Mixed coal combustion and vehicle emission	Industrial processes	Biomass burning

Rotation method: Varimax with Kaiser Normalization.
Factor loadings higher than 0.90 were shown in bold. For those lower than 0.90, the three species with higher loading values are stamped in bold.

3.3.2. PCA results

PCA was firstly run for different rings of PAHs, to see the differences of sources and environmental behaviors of them. From Table 6, it can be found that 2-ring and 3-ring PAHs are clearly extracted for both of the two sites, which indicates that the sources and environmental behaviors of them are different from other rings of PAHs. The result is similar with that for the correlation analysis as listed in Table 3.

For PAH species, the PCA factor loadings are presented in Table 7 with three factors extracted, totally explaining 92.2% and 84% of the variance respectively. For both BM and SC, factor 1 has higher loadings of Ant, Ace, Fl, Flu, Pyr, BaA, BkF, BaP, BeP, DBA, InP, BghiP and Cor. In Jamhari et al. (2014), factor 1 with high loadings of Flu, Pyr, BaA and Chr was regarded as natural gas and coal combustion. High molecular weight PAHs, such as BaP, BeP, InP, DBA, BghiP and Cor, were widely used as tracers for gasoline and diesel exhaust (Chang et al., 2006; Omar et al., 2006; Wang et al., 2008; Lai et al., 2013; Wu et al., 2014b). Therefore, factor 1 can be regarded as the mixing of coal combustion and vehicle emission, explaining 67% and 55.4% of the total variance at BM and SC, respectively. For factor 2 at BM, it explained 17.3% of the total variance, with higher loadings of Flu, Chr and BbF. For factor 3 at SC, it explained 6.7% of the variance, with higher loadings of Ant and BkF. These two factors could be regarded as biomass burning as during summer and autumn period, agricultural waste burning activities are frequently occurred in China. Yang et al. (2006) found that at rice straw burning period Flu, Pyr and Ant were 3–5 times of those for non-burning days. Hays et al. (2003) obtained that Ace, BaP, BbF and BkF emitted from wood combustion held higher emission factors. For factor 3 of BM, it explained 7.8% of the variance, highly weighted with NaP and Ace, which was related with joss paper burning (Lai et al., 2013) at the temples of Mt. Huang. Factor 2 of SC, with higher loadings of NaP, Acy, Fl and Phe, can be recognized as industrial activities as they were markers for stationary sources in China with coal as fuel (Kong et al., 2011, 2013).

It should be emphasized that for source identification of PAHs in fine particles by diagnostic ratios and PCA, the results are both qualitative or semi-quantitative (Galarneau, E., 2008; Gao et al., 2012). Local source profiles are needed to obtain more reasonable and accurate source identification results (Galarneau, E., 2008; Ravindra et al., 2008; Gao et al., 2012; Kong et al., 2013). And also current diagnostic ratios and markers used in literatures are quite old and needed urgent update especially for PAHs in $PM_{2.5}$ emitted from various sources in China (Kong et al., 2013).

3.4. Health risk assessment for construction workers

The total BaP equivalents (BaPeq) determined by toxic equivalent factors (TEF) and the concentrations of individual PAHs were listed in Fig. 7a. BaPeq was 1.3 ng m^{-3} at SC, nearly ten times of that at BM, reflecting highly elevated health risks for workers exposed to PAHs at the subway construction site.

The estimated ILCR for construction workers exposed to PAHs at SC reached 0.6 per 1,000,000 exposed workers (Fig. 7b), close to the acceptable levels of 10^{-6} to 10^{-4} (Jamhari et al., 2014). The guideline value for ambient BaP is 1.0 ng m^{-3} in China, thus the acceptable risk of exposure to PAHs via inhalation is 10^{-6}. In this study, the BaP concentrations were in the range of 0.2–2.0 ng m^{-3}, implying that the cancer risks of construction workers exposed to PAHs in $PM_{2.5}$ should be paid attention.

4. Conclusion

Mass concentrations, sources and health risks of PAHs in $PM_{2.5}$ at a subway construction site (SC) of Nanjing were studied, and compared with the regional background mountainous site (BM)—Mt. Huang. The average PAH concentration in $PM_{2.5}$ at SC was 9.02 ng m^{-3}, 5.9 times higher than that at BM (1.53 ng m^{-3}). All PAH species were higher at SC, with the SC/BM ratios ranging from 1.3 (NaP) to 10.3 (BaP). Coefficient of divergence value indicated that PAH profiles were different for the two sites, influenced by the higher mass percentages of PAHs from different sources and by different meteorological parameters, especially for temperature. The ratios of PAHs (3 + 4 ring)/PAHs (5 + 6 ring) and BaP/BeP indicated that PAHs at BM may suffer from more enhanced photochemical degradation processes. Diagnostic ratios and principal component analysis indicated that coal combustion, traffic emissions and biomass burning were the coexisting sources for PAHs at both SC and BM, accounting for 62.1% and 84.3% of the variance in total, respectively. Owing to the different surrounding environments, PAHs were influenced by specific sources, which were joss paper burning at BM and industrial activities at SC. The construction workers are exposed to higher BaPeq concentrations, nearly ten times of the background site and their lifetime cancer risks reached 0.6 per 1,000,000 exposed worker. Effective measures should be established to control the fine particle emissions from various construction activities, such as road dust, non-road engines and on-road vehicle exhausts. With limitation on sampling equipment, collecting of particles at the two sites is not synchronously conducted. In the future, the seasonal and spatial variation of PAHs in fine particles at Yangtze River Delta region should be considered and well designed.

Acknowledgment

This work was funded by the National Natural Science Foundation of China (No. 41030962 and No. 41305119), the Priority Academic Program Development (PAPD) of Jiangsu Higher Education Institution, the Research Fund for Jiangsu Higher Education Institutions (13KJB170010), and the Research Fund for Environmental Protection of Jiangsu Province (2014050).

References

Bi, X.H., Sheng, G.Y., Peng, P.A., Zhang, Z.Q., Fu, J.M., 2002. Extractable organic matter in PM_{10} from LiWan district of Guangzhou City, PR China. Sci. Total Environ. 300, 213–228.

Bi, X.H., Sheng, G.Y., Peng, P.A., Chen, Y.J., Fu, J.M., 2005. Size distribution of n-alkanes and polycyclic aromatic hydrocarbons (PAHs) in urban and rural atmospheres of Guangzhou, China. Atmos. Environ. 39, 477–487.

Bourotte, C., Fortic, M.C., Taniguchi, S., Bıcego, M.C., Lotufo, P.A., 2005. A wintertime study of PAHs in fine and coarse aerosols in Sao Paulo city, Brazil. Atmos. Environ. 39, 3799–3811.

Chang, K.F., Fang, G.C., Chen, J.C., Wu, Y.S., 2006. Atmospheric polycyclic aromatic hydrocarbons (PAHs) in Asia: a review from 1999 to 2004. Environ. Pollut. 142, 388–396.

Chen, F., Hu, W., Zhong, Q., 2013. Emissions of particle-phase polycyclic aromatic hydrocarbons (PAHs) in the Fu Gui-shan Tunnel of Nanjing, China. Atmos. Res. 124, 53–60.

Chen, K., Yin, Y., Kong, S., Xiao, H., Wu, Y., Chen, J., Li, A., 2014. Size-resolved chemical composition of atmospheric particles during a straw burning period at Huangshan (the Yellow Mountain) of China. Atmos. Environ. 84, 380–389.

Choi, S.D., Shunthirasingham, C., Daly, G.L., Xiao, H., Lei, Y.D., Wania, F., 2009. Levels of polycyclic aromatic hydrocarbons in Canadian mountain air and soil are controlled by proximity to roads. Environ. Pollut. 157, 3199–3206.

Deng, J.J., Xing, Z.Y., Zhuang, B.L., Du, K., 2014. Comparative study on long-term visibility trend and its affecting factors on both sides of the Taiwan Strait. Atmos. Res. 143, 266–278.

Ding, A.J., Fu, C.B., Yang, X.Q., Sun, J.N., Zheng, L.F., Xie, Y.N., Herrmann, E., Nie, W., Petäjä, T., Kerminen, V.M., Kulmala, M., 2013. Ozone and fine particle in the western Yangtze River Delta: an overview of 1 yr data at the SORPES station. Atmos. Chem. Phys. 13, 5813–5830.

Duan, J.C., Bi, X.H., Tan, J.H., Sheng, G.Y., Fu, J.M., 2005. The differences of the size distribution of polycyclic aromatic hydrocarbons (PAHs) between urban and rural sites of Guangzhou, China. Atmos. Res. 78, 190–203.

Duan, J.C., Bi, X.H., Tan, J.H., Sheng, G.Y., Fu, J.M., 2007. Seasonal variation on size distribution and concentration of PAHs in Guangzhou city, China. Chemosphere 67, 614–622.

Elghawi, U.M., Mayouf, A., Tsolakis, A., Wyszynski, M.L., 2010. Vapour-phase and particulate-bound PAHs profile generated by a (SI/HCCI) engine from a winter grade commercial gasoline fuel. Fuel 89, 2019–2025.

Esen, F., Tasdemir, Y., Vardar, N., 2008. Atmospheric concentrations of PAHs, their possible sources and gas-to-particle partitioning at a residential site of Bursa, Turkey. Atmos. Res. 88, 243–255.

Filippo, P.D., Riccardi, C., Pomata, D., Buiarelli, F., 2010. Concentrations of PAHs, and nitro- and methyl-derivatives associated with size-segregated urban aerosol. Atmos. Environ. 44, 2742–2749.
Galarneau, E., 2008. Source specificity and atmospheric processing of airborne PAHs: implications for source apportionment. Atmos. Environ. 42, 8139–8149.
Gao, B., Guo, H., Wang, X.M., Zhao, X.Y., Ling, Z.H., Zhang, Z., Liu, T.Y., 2012. Polycyclic aromatic hydrocarbons in $PM_{2.5}$ in Guangzhou, southern China: spatiotemporal patterns and emission sources. J. Hazard. Mater. 239–240, 78–87.
Gao, B., Yu, J.Z., Li, S.X., Ding, X., He, Q.F., Wang, X.M., 2011. Roadside and rooftop measurements of polycyclic aromatic hydrocarbons in $PM_{2.5}$ in urban Guangzhou: evaluation of vehicular and regional combustion source contributions. Atmos. Environ. 45, 7184–7191.
Geng, N.B., Wang, J., Xu, Y.F., Zhang, W.D., Chen, C., Zhang, R.Q., 2013. $PM_{2.5}$ in an industrial district of Zhengzhou, China: chemical composition and source apportionment. Particuology 11, 99–109.
Gu, Z.P., Feng, J.L., Han, W.L., Li, L., Wu, M.H., Fu, J.M., Sheng, G.Y., 2010. Diurnal variations of polycyclic aromatic hydrocarbons associated with $PM_{2.5}$ in Shanghai, China. J. Environ. Sci. 3, 389–396.
Han, B., Bai, Z.P., Guo, G.H., Wang, F., Li, F., Liu, Q.X., Ji, Y.Q., Li, X., Hu, Y.D., 2009. Characterization of PM_{10} fraction of road dust for polycyclic aromatic hydrocarbons (PAHs) from Anshan, China. J. Hazard. Mater. 170, 934–940.
Hays, M.D., Smith, N.D., Kinsey, J., Dong, Y., Kariher, P., 2003. Polycyclic aromatic hydrocarbon size distributions in aerosols from appliances of residential wood combustion as determined by direct thermal desorption–GC/MS. Aerosol Sci. 34, 1061–1084.
Hart, K.M., Pankow, J.F., 1990. Comparison of n-Alkane and PAH concentrations collected on quartz fiber and teflon membrane filters in an urban environment. J. Aerosol Sci. 21, S377–S380.
Hassanien, M.A., Latif, N.M.A., 2008. Polycyclic aromatic hydrocarbons in road dust over Greater Cairo, Egypt. J. Hazard. Mater. 151, 247–254.
He, J.B., Fan, S.X., Meng, Q.Z., Sun, Y., Zhang, J., Zu, F., 2014. Polycyclic aromatic hydrocarbons (PAHs) associated with fine particulate matters in Nanjing, China: distributions, sources and meteorological influences. Atmos. Environ. 89, 207–215.
Hong, H.S., Yin, H.L., Wang, X.H., Ye, C.X., 2007. Seasonal variation of PM_{10}-bound PAHs in the atmosphere of Xiamen, China. Atmos. Res. 85, 429–441.
Hu, J., Liu, C.Q., Zhang, G.P., Zhang, Y.L., 2012. Seasonal variation and source apportionment of PAHs in TSP in the atmosphere of Guiyang, Southwest China. Atmos. Res. 118, 271–279.
Huang, X.F., He, L.Y., Hu, M., Zhang, Y.H., 2006. Annual variation of particulate organic compounds in $PM_{2.5}$ in the urban atmosphere of Beijing. Atmos. Environ. 40, 2449–2458.
Jamhari, A.A., Sahani, M., Latif, M.T., Chan, K.M., Tan, H.S., Khan, M.F., Tahir, N.M., 2014. Concentration and source identification of polycyclic aromatic hydrocarbons (PAHs) in PM_{10} of urban, industrial and semi-urban areas in Malaysia. Atmos. Environ. 86, 16–27.
Kavouras, I.G., Lawrence, J., Koutrakis, P., Stephanou, E.G., Oyola, P., 1999. Measurement of particulate aliphatic and polynuclear aromatic hydrocarbons in Santiago de Chile: source reconciliation and evaluation of sampling artifacts. Atmos. Environ. 33, 4977–4986.
Khalili, N.R., Scheff, P.A., Holsen, T.M., 1995. PAH source fingerprints for coke ovens, diesel and gasoline engines, highway tunnels, and wood combustion emissions. Atmos. Environ. 29, 533–542.
Kong, S.F., Shi, J.W., Lu, B., Qiu, W.G., Zhang, B.S., Peng, Y., Bai, Z.P., 2011. Characterization of PAHs within PM_{10} fraction for ashes from coke production, iron smelt, heating station and power plant stacks in Liaoning Province, China. Atmos. Environ. 45, 3777–3785.
Kong, S.F., Ji, Y.Q., Li, Z.Y., Lu, B., Bai, Z.P., 2013. Emission and profile characteristic of polycyclic aromatic hydrocarbons in PM_{10} and $PM_{2.5}$ from stationary sources based on dilution sampling. Atmos. Environ. 77, 155–165.
Kong, S.F., Lu, B., Ji, Y.Q., Bai, Z.P., Xu, Y.H., Liu, Y., Jiang, H., 2012. Distribution and sources of polycyclic aromatic hydrocarbons in size-differentiated re-suspended dust on building surfaces in an oilfield city, China. Atmos. Environ. 55, 7–16.
Ladji, R., Yassaa, N., Balducci, C., Cecinato, A., Meklati, B.Y., 2009. Distribution of the solvent-extractable organic compounds in fine (PM_1) and coarse (PM_{1-10}) particles in urban, industrial and forest atmospheres of Northern Algeria. Sci. Total Environ. 408, 415–424.
Lai, I., Chang, Y.C., Lee, C.L., Chiou, G.Y., Huang, H.C., 2013. Source identification and characterization of atmospheric polycyclic aromatic hydrocarbons along the southwestern coastal area of Taiwan with a GMDH approach. J. Environ. Manag. 115, 60–68.
Lammel, G., Klánová, J., Kohoutek, J., Prokeš, R., Ries, L., Stohl, A., 2009. Observation and origin of organochlorine compounds and polycyclic aromatic hydrocarbons in the free troposphere over central Europe. Environ. Pollut. 157, 3264–3271.
Lee, J.Y., Kim, Y.P., Kaneyasu, N., Kumata, H., Kang, C.H., 2008. Particulate PAHs levels at Mt. Halla site in Jeju Island, Korea: regional background levels in northeast Asia. Atmos. Res. 90, 91–98.
Lee, S.C., Ho, K.F., Chan, L.Y., Zielinska, B., Chow, J.C., 2001. Polycyclic aromatic hydrocarbons (PAHs) and carbonyl compounds in urban atmosphere of Hong Kong. Atmos. Environ. 35, 5949–5960.
Leung, P.Y., Wan, H.T., Billah, M.B., Cao, J.J., Ho, K.F., Wong, C.K.C., 2014. Chemical and biological characterization of air particulate matter 2.5, collected from five cities in China. Environ. Pollut. 194, 188–195.
Li, Y.S., Cao, J.J., Li, J.J., Zhou, J.M., Xu, H.M., Zhang, R.J., Ouyang, Z.Y., 2013a. Molecular distribution and seasonal variation of hydrocarbons in $PM_{2.5}$ from Beijing during 2006. Particuology 11, 78–85.
Li, C.L., Fu, J.M., Sheng, G.Y., Bi, X.H., Hao, Y.M., Wang, X.M., Mai, B.X., 2005. Vertical distribution of PAHs in the indoor and outdoor $PM_{2.5}$ in Guangzhou, China. Build. Environ. 40, 329–341.
Li, P.H., Kong, S.F., Geng, C.M., Han, B., Lu, B., Sun, R.F., Zhao, R.J., Bai, Z.P., 2013b. Health risk assessment for vehicle inspection workers exposed to airborne polycyclic aromatic hydrocarbons (PAHs) in their work place. Environ. Sci.: Processes Impacts 3, 623–632.
Li, R.J., Kou, X.J., Geng, H., Dong, C., Cai, Z.W., 2014a. Pollution characteristics of ambient $PM_{2.5}$-bound PAHs and NPAHs in a typical winter time period in Taiyuan. Chinese Chem. Lett. 25, 663–666.
Li, W., Wang, C., Wang, H.Q., Chen, J.W., Shen, H.Z., Shen, G.F., Huang, Y., Wang, R., Wang, B., Zhang, Y.Y., Chen, H., Chen, Y.C., Su, S., Lin, N., Tang, J.H., Li, Q.B., Wang, X.L., Liu, J.F., Tao, S., 2014b. Atmospheric polycyclic aromatic hydrocarbons in rural and urban areas of northern China. Environ. Pollut. 192, 83–90.
Li, J.J., Wang, G.H., Zhou, B.H., Cheng, C.L., Cao, J.J., Shen, Z.X., An, Z.S., 2012. Airborne particulate organics at the summit (2060 m, a.s.l.) of Mt. Hua in central China during winter: implications for biofuel and coal combustion. Atmos. Res. 106, 108–119.
Liang, F., Lu, M.M., Birch, M.E., Keener, T.C., Liu, Z.F., 2006. Determination of polycyclic aromatic sulfur heterocycles in diesel particulate matter and diesel fuel by gas chromatography with atomic emission detection. J. Chromatogr. A 1114, 145–153.
Liu, N.W., Ma, Y.J., Ma, J.Z., Wang, Y.F., Yang, S.Y., Li, L.G., 2015. Atmospheric extinction properties in Shenyang, China. Particuology 18, 120–126.
Ma, W.L., Li, Y.F., Qi, H., Sun, D.Z., Liu, L.Y., Wang, D.G., 2010. Seasonal variations of sources of polycyclic aromatic hydrocarbons (PAHs) to a northeastern urban city, China. Chemosphere 79, 441–447.
Ma, W.L., Sun, D.Z., Shen, W.G., Yang, M., Qi, H., Liu, L.Y., Shen, J.M., Li, Y.F., 2011. Atmospheric concentrations, sources and gas–particle partitioning of PAHs in Beijing after the 29th Olympic Games. Environ. Pollut. 159, 1794–1801.
Mandalakis, M., Tsapakis, M., Tsoga, A., Stephanou, E.G., 2002. Gas–particle concentrations and distribution of aliphatic hydrocarbons, PAHs, PCBs and PCDD/Fs in the atmosphere of Athens (Greece). Atmos. Environ. 36, 4023–4035.
Mader, B., Pankow, J.F., 2001. Gas/solid partitioning of semivolatile organic compounds (SOCs) to air filters. 3. An analysis of gas adsorption artifacts in measurements of atmospheric SOCs and organic carbon (OC) when using teflon membrane filters and quartz fiber filters. Environ. Sci. Technol. 17, 3422–3431.
Masiol, M., Formenton, G., Pasqualetto, A., Pavoni, B., 2013. Seasonal trends and spatial variations of PM_{10}-bounded polycyclic aromatic hydrocarbons in Veneto Region, Northeast Italy. Atmos. Environ. 79, 811–821.
Mu, L., Pen, L., Liu, X.F., Song, C.F., Bai, H.L., Zhang, J.Q., Hu, D.M., He, Q.S., Li, F., 2014. Characteristics of polycyclic aromatic hydrocarbons and their gas/particle partitioning from fugitive emissions in coke plants. Atmos. Environ. 83, 202–210.
Murakami, M., Nakajima, F., Furumai, H., 2005. Size- and density-distributions and sources of polycyclic aromatic hydrocarbons in urban road dust. Chemosphere 61, 783–791.
Okuda, T., Kumata, H., Naraoka, H., Takada, H., 2002. Origin of atmospheric polycyclic aromatic hydrocarbons (PAHs) in Chinese cities solved by compound-specific stable carbon isotopic analyses. Org. Geochem. 33, 1737–1745.
Okuda, T., Matsuura, S., Yamaguchi, D., Umemura, T., Hanada, E., Orihara, H., Tanaka, S., He, K.B., Ma, Y.L., Cheng, Y., Liang, L.L., 2011. The impact of the pollution control measures for the 2008 Beijing Olympic Games on the chemical composition of aerosols. Atmos. Environ. 45, 2789–2794.
Okuda, T., Naoi, D., Tenmoku, M., Tanaka, S., He, K.B., Ma, Y.L., Yang, F.M., Lei, Y., Jia, Y.T., Zhang, D.H., 2006. Polycyclic aromatic hydrocarbons (PAHs) in the aerosol in Beijing, China, measured by aminopropylsilane chemically-bonded stationary-phase column chromatography and HPLC/fluorescence detection. Chemosphere 65, 427–435.
Omar, N.Y.M.J., Mon, T.C., Rahman, N.A., Abas, M.R.B., 2006. Distributions and health risks of polycyclic aromatic hydrocarbons (PAHs) in atmospheric aerosols of Kuala Lumpur, Malaysia. Sci. Total Environ. 369, 76–81.
Possanzini, M., Palo, V.D., Gigliucci, P., Scianò, M.C.T., Cecinato, A., 2004. Determination of phase-distributed PAH in Rome ambient air by denuder/GC–MS method. Atmos. Environ. 38, 1727–1734.
Rau, J.Y., Tseng, H.H., Lin, M.D., Wey, M.Y., Lin, Y.H., Chu, C.W., Lee, C.H., 2008. Characterization of polycyclic aromatic hydrocarbon emission from open burning of joss paper. Atmos. Environ. 42, 1692–1701.
Ravindra, K., Sokhi, R., Grieken, R.V., 2008. Atmospheric polycyclic aromatic hydrocarbons: Source attribution, emission factors and regulation. Atmos. Environ. 42, 2895–2921.
Shen, G.F., Wei, S.Y., Zhang, Y.Y., Wang, B., Wang, R., Shen, H.Z., Li, W., Huang, Y., Chen, Y.C., Chen, H., Tao, S., 2013. Emission and size distribution of particle-bound polycyclic aromatic hydrocarbons from residential wood combustion in rural China. Biomass Bioenergy 55, 141–147.
Shi, G.L., Liu, G.R., Tian, Y.Z., Zhou, X.Y., Peng, X., Feng, Y.C., 2014. Chemical characteristic and toxicity assessment of particle associated PAHs for the short-term anthropogenic activity event: during the Chinese New Year's Festival in 2013. Sci. Total Environ. 482–483, 8–14.
Sun, J.L., Jing, X., Chang, W.J., Chen, Z.X., Zeng, H., 2015. Cumulative health risk assessment of halogenated and parent poly-cyclic aromatic hydrocarbons associated with particulate matters in urban air. Ecotoxicol. Environ. Saf. 113, 31–37.
Subramanyam, V., Valsaraj, K.T., Thibodeaux, L.J., Reible, D.D., 1994. Gas-to-particle partitioning of polycyclic aromatic hydrocarbons in an urban atmosphere. Atmos. Environ. 19, 3083–3091.
Tan, J.H., Bi, X.H., Duan, J.C., Rahn, K.A., Sheng, G.Y., Fu, J.M., 2006. Seasonal variation of particulate polycyclic aromatic hydrocarbons associated with PM_{10} in Guangzhou, China. Atmos. Res. 80, 250–262.

Tan, J.H., Guo, S.J., Ma, Y.L., Duan, J.C., Cheng, Y., He, K.B., Yang, F.M., 2011. Characteristics of particulate PAHs during a typical haze episode in Guangzhou, China. Atmos. Res. 102, 91–98.
Tan, J.H., Duan, J.C., Chen, D.H., Wang, X.H., Guo, S.J., Bi, X.H., Sheng, G.Y., He, K.B., Fu, J.M., 2009. Chemical characteristics of haze during summer and winter in Guangzhou. Atmos. Res. 94, 238–245.
Tao, J., Gao, J., Zhang, L., Zhang, R., Che, H., Zhang, Z., Lin, Z., Jing, J., Cao, J., Hsu, S.C., 2014. $PM_{2.5}$ pollution in a megacity of southwest China: source apportionment and implication. Atmos. Chem. Phys. 14, 8679–8699.
Tao, S., Wang, Y., Wu, S.M., Liu, S.Z., Dou, H., Liu, Y.N., Lang, C., Hu, F., Xing, B.S., 2007. Vertical distribution of polycyclic aromatic hydrocarbons in atmospheric boundary layer of Beijing in winter. Atmos. Environ. 41, 9594–9602.
Tsapakis, M., Stephanou, E.G., 2003. Collection of gas and particle semi-volatile organic compounds: use of an oxidant denuder to minimize polycyclic aromatic hydrocarbons degradation during high-volume air sampling. Atmos. Environ. 37, 4935–4944.
Vardar, N., Tasdemir, Y., Odabasi, M., Noll, K.E., 2004. Characterization of atmospheric concentrations and partitioning of PAHs in the Chicago atmosphere. Sci. Total Environ. 327, 163–174.
Wang, H., Tan, S.C., Wang, Y., Jiang, C., Shi, G.Y., Zhang, M.X., Che, H.Z., 2014. A multisource observation study of the severe prolonged regional haze episode over eastern China in January 2013. Atmos. Environ. 89, 807–815.
Wang, P., Cao, J.J., Shen, Z.X., Han, Y.M., Lee, S.C., Huang, Y., Zhu, C.S., Wang, Q.Y., Xu, H.M., Huang, R.J., 2015a. Spatial and seasonal variations of $PM_{2.5}$ mass and species during 2010 in Xi'an, China. Sci. Total Environ. 508, 477–487.
Wang, G., Kawamura, K., Xie, M., Hu, S., Gao, S., Cao, J., An, Z., Wang, Z., 2009. Size-distributions of n-alkanes, PAHs and hopanes and their sources in the urban, mountain and marine atmospheres over East Asia. Atmos. Chem. Phys. 9, 8869–8882.
Wang, G.H., Huang, L.M., Zhao, X., Niu, H.Y., Dai, Z.X., 2006. Aliphatic and polycyclic aromatic hydrocarbons of atmospheric aerosols in five locations of Nanjing urban area, China. Atmos. Res. 81, 54–66.
Wang, J., Li, X., Jiang, N., Zhang, W.K., Zhang, R.Q., Tang, X.Y., 2015b. Long term observations of $PM_{2.5}$-associated PAHs: comparisons between normal and episode days. Atmos. Environ. 104, 228–236.
Wang, X.F., Cheng, H.X., Xu, X.B., Zhuang, G.M., Zhao, C.D., 2008. A wintertime study of polycyclic aromatic hydrocarbons in $PM_{2.5}$ and $PM_{2.5-10}$ in Beijing: assessment of energy structure conversion. J. Hazard. Mater. 157, 47–56.
Wang, W.T., Simonich, S.L.M., Wang, W., Giri, B., Zhao, J.Y., Xue, M., Cao, J., Lu, X.X., Tao, S., 2011. Atmospheric polycyclic aromatic hydrocarbon concentrations and gas/particle partitioning at background, rural village and urban sites in the North China Plain. Atmos. Res. 99, 197–206.
Wiriya, W., Prapamontol, T., Chantara, S., 2013. PM_{10}-bound polycyclic aromatic hydrocarbons in Chiang Mai (Thailand): seasonal variations, source identification, health risk assessment and their relationship to air-mass movement. Atmos. Res. 124, 109–122.
Wu, S.P., Tao, S., Zhang, Z.H., Lan, T., Zuo, Q., 2005. Distribution of particle-phase hydrocarbons, PAHs and OCPs in Tianjin, China. Atmos. Environ. 39, 7420–7432.
Wu, D., Wang, Z.S., Chen, J.H., Kong, S.F., Fu, X., Deng, H.B., Shao, G.F., Wu, G., 2014a. Polycyclic aromatic hydrocarbons (PAHs) in atmospheric $PM_{2.5}$ and PM_{10} at a coal-based industrial city: implication for PAH control at industrial agglomeration regions, China. Atmos. Res. 149, 217–229.
Wu, Y., Yang, L., Zheng, X., Zhang, S.J., Song, S.J., Li, J.Q., Hao, J.M., 2014b. Characterization and source apportionment of particulate PAHs in the roadside environment in Beijing. Sci. Total Environ. 470–471, 76–83.
Xia, Z.H., Duan, X.L., Tao, S., Qiu, W.X., Liu, D., Wang, Y.L., Wei, S.Y., Wang, B., Jiang, Q.J., Lu, B., Song, Y.X., Hu, X.X., 2013. Pollution level, inhalation exposure and lung cancer risk of ambient atmospheric polycyclic aromatic hydrocarbons (PAHs) in Taiyuan, China. Environ. Pollut. 173, 150–156.
Yang, H.H., Chiang, C.F., Lee, W.J., Hwang, K.P., Wu, E.M.Y., 1999. Size distribution and dry deposition of road dust PAHs. Environ. Int. 25, 585–597.
Yang, H.H., Lai, S.O., Hsieh, L.T., Hsueh, H.J., Chi, T.W., 2002. Profiles of PAH emission from steel and iron industries. Chemosphere 48, 1061–1074.
Yang, H.H., Lee, W.J., Chen, S.J., Lai, S.O., 1998. PAH emission from various industrial stacks. J. Hazard. Mater. 60, 159–174.
Yang, H.H., Lee, W.J., Theen, L.J., Kua, C.W., 1997. Particle size distribution and PAH content of road dust. J. Aerosol Sci. 28, S125–S126.
Yang, H.H., Tsai, C.H., Chao, M.R., Su, Y.L., Chien, S.M., 2006. Source identification and size distribution of atmospheric polycyclic aromatic hydrocarbons during rice straw burning period. Atmos. Environ. 40, 1266–1274.
Zhang, F.W., Xu, L.L., Chen, J.S., Chen, X.Q., Niu, Z.C., Lei, T., Li, C.M., Zhao, J.P., 2013a. Chemical characteristics of PM2.5 during haze episodes in the urban of Fuzhou, China. Particuology 11, 264–272.
Zhang, L.F., Zhang, T., Dong, L., Shi, S.X., Zhou, L., Huang, Y.R., 2013b. Assessment of halogenated POPs and PAHs in three cities in the Yangtze River Delta using high-volume samplers. Sci. Total Environ. 454–455, 619–626.
Zhao, H.T., Yin, C.Q., Chen, M.X., Wang, W.D., Jefferies, C., Shan, B.Q., 2009. Size distribution and diffuse pollution impacts of PAHs in street dust in urban streams in the Yangtze River Delta. J. Environ. Sci. 21, 162–167.
Zhao, P.S., Dong, F., He, D., Zhao, X.J., Zhang, X.L., Zhang, W.Z., Yao, Q., Liu, H.Y., 2013. Characteristics of concentrations and chemical compositions for $PM_{2.5}$ in the region of Beijing, Tianjin, and Hebei, China. Atmos. Chem. Phys. 13, 4631–4644.
Zhou, J.B., Wang, T.G., Huang, Y.B., Mao, T., Zhong, N.N., 2005. Size distribution of polycyclic aromatic hydrocarbons in urban and suburban sites of Beijing, China. Chemosphere 61, 792–799.